



# Vibration welding of components with angled areas in the direction of vibration

Sascha Vogtschmidt<sup>1</sup> · Isabel Fiebig<sup>1</sup> · Volker Schoeppner<sup>1</sup>

Received: 8 December 2019 / Accepted: 15 July 2020 / Published online: 24 July 2020  
© The Author(s) 2020

## Abstract

Conventional manufacturing processes for plastic products, such as injection molding or extrusion, often limit the achievable component geometries. Therefore, it is necessary to join components in order to generate highly complex geometries. Vibration welding is one way of joining components. This process is frequently used and is characterized by short cycle times, high energy efficiency, and the possibility of joining large components. In vibration welding, plastic components are heated by an oscillating friction movement of the joining surfaces, then plasticized and subsequently welded together. The joining of three-dimensional seam geometries is therefore a challenge for vibration welding, as the components can be lifted off by the linear movement and the surfaces do not plasticize sufficiently. Previous investigations have shown that angles of up to 20° can be welded in the direction of vibration, but that the deviation from the plane considerably reduces the weld strength. In order to weld three-dimensional weld seam geometries with short cycle times and simultaneously achieve a high weld seam strength, a process is being developed which is intended to extend the design freedom in vibration welding.

**Keywords** Vibration welding · Infrared welding · Polymer joining

## 1 Introduction

The welding of plastics is often one of the last process steps in the production of plastic products and enables the realization of geometries and functions that cannot be achieved by injection molding and extrusion. The joining processes essentially define the component design. In the often design-oriented products, these geometries partly represent a major limitation, especially when joining processes with short cycle times have

to be selected from an economic point of view. In the development of new products, it makes sense to use a joining process that is flexible and suitable for complex geometries. In the group of plastic welding processes, only hot plate welding and infrared welding offer the necessary degrees of freedom [1, 2] for three-dimensional joining surfaces. In addition to the feasibility of the joining geometry, the cycle time is a decisive factor. In this case, hot plate and IR welding have deficiencies compared with other methods such as ultrasonic and vibration welding.

---

Recommended for publication by Commission XVI - Polymer Joining and Adhesive Technology

---

✉ Sascha Vogtschmidt  
sascha.vogtschmidt@ktp.upb.de

Isabel Fiebig  
isabel.fiebig@ktp.upb.de

Volker Schoeppner  
volker.schoeppner@ktp.upb.de

<sup>1</sup> Kunststofftechnik Paderborn, Paderborn University, Paderborn, Germany

## 2 Motivation

The requirements for complex weld seam arrangements and cycle times collide in currently available plastic welding processes. For example, fast welding processes such as ultrasonic or vibration welding is frequently used. A major disadvantage is the limited freedom of these welding processes with regard to the weld geometry. In ultrasonic welding, it is necessary to place the joining surface perpendicular to the sonotrode axis and parallel to the sonotrode surface, because the position and

design have a decisive influence on the weld seam quality. Vibration welding has the disadvantage of limited design freedom with regard to three-dimensional seam structures, as the relative movement for the energy input during vibration welding occurs in one plane. Generally, the relative movement is parallel to the joining surface. In the case of deviations from the flat joining surface, the energy input is not optimal, which limits the process to small partial inclinations [1, 2].

If the joining planes of the components do not lie in the direction of the vibration movement during vibration welding, the shearing movement is superimposed, which can lead to the joining partners being lifted off. For this reason, processes with longer cycle times are currently being selected for complex weld seam geometries.

Due to the energy supply via heat conduction, hot plate welding is a much slower joining process than ultrasonic or vibration welding, even if an attempt is made to shorten the cooling time by convection. In addition, a low-viscosity melt can adhere to the heating element and reduce the quality of the weld seam, so that hot plate welding is only of limited use for low-viscosity materials. [2–6].

The aim of these investigations was to develop a new welding process that allows the welding of large deviations from the joining plane for design-oriented products in short cycle times. The idea was to develop an alternating expansion welding process which dissipates energy into a thin molten film which was plasticized by infrared radiation, and in this way, a complete weld seam can be formed in a short cycle time. The plasticizing process continues due to a superposition of shear and strain dissipation. The process is shown schematically in Fig. 1. Due to the similarity of this process to vibration welding, these processes can be combined in one process step. As a result, the previous process limits of vibration welding are overcome and the design freedom of the designer is hardly restricted in the arrangement of the joining zone. The research project aims to combine the process requirements of high design freedom with process times.

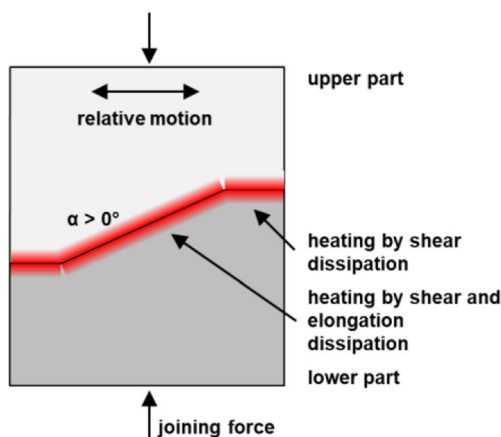


Fig. 1 Schematic illustration of the process

## 2.1 Vibration welding

The scientific analysis of vibration welding started very early [7–11]. The welding process is based on plastic melting by friction of the joining partners on each other, whereby the energy transformation is proportional to the average friction speed. The basic principle of vibration welding is the introduction of heat by shear dissipation. Linear vibration welding is the form of vibration welding with the most frequent application. In addition to linear oscillation, orbital oscillation is used in industrial practice. The mechanical properties and morphology of vibration-welded components are the subject of various publications [7–9, 12, 13] in addition to process comparisons. Linear and orbital vibration welding are theoretically understood; concepts for pressure-staged process control, process automation, and quality assurance are available [14], whereby the work was published mainly in Germany (LKT, IKV, KTP) and in North America (Bates, Wu). The German Welding Society (DVS) guidelines provide the user with information on process design [15].

Previous investigations have shown that vibration welding can be used to produce high-quality welds. The quality of a weld seam is often described by the weld factor. This factor relates the strength of the weld to the strength of the base material. This relationship is shown in the following equation:

$$f_w = \frac{\sigma_w}{\sigma_m}$$

The aim of every welding process is to generate the highest possible welding factor so that the weld seam of the resulting component is not a critical point. The welding factor of 1 means that the weld has the same strength as the base material. Tests already carried out have shown that welding factors of 1 could be determined for vibration welds made of polypropylene and polyamide [10, 16] and welding factors of 0.85 for welds made of PC-ABS [17]. Despite the high level of process understanding, the high weld strengths are often not achieved in industrial series production [18, 19]. Besides different wall thicknesses, component distortion, and different vibration directions, deviations of the joining zone from the vibration plane are also responsible for this. In these areas, the energy input via shear dissipation can only take place to a limited extent and insufficient weld seams of low strength are the result. According to relevant guidelines, only deviations < 10° from the vibration plane can be successfully welded [15]. Furthermore, Bates et al. showed that with increasing angle of the deviations from the vibration plane, vibration welding could be performed, but decreasing weld strengths were registered in these areas [18, 19]. For example, an increase in the joining angle from 0 to 20° for glass fiber-reinforced polyamide 6 resulted in a 50% reduction in strength.

## 2.2 Infrared welding

Infrared welding has significant advantages compared with other welding processes. For example, there is no contact between the component and the heat source and the radiator can be switched on and off in a process-controlled manner. Contactless preheating is used to prevent particle output during vibration welding in order to generate a melt film before the vibration starts [3, 4, 20–22]. In vibration welding with infrared preheating, the heat is generated at the beginning of the process by pure radiant heating. Infrared welding can be used to create joints of high strength. Previous investigations have shown that infrared welding factors above 0.9 can be achieved for most materials [23].

## 2.3 Dissipation heating

The physical dissipation energy used in these investigations for the rapid joining of three-dimensional geometries describes the energy converted into heat. It leads to a further heating of the preplasticized melt, with the friction having the largest part. The heating takes place due to the shear flow caused by the squeezing flow and the vibrating movement. In the case of high-molecular liquids such as plastic melt, a large proportion of the energy used for the flow movement is converted into heat [24, 25].

## 3 Experimental setup

The investigations concerning vibration welding with angled areas in the direction of vibration are generally divided into two areas. The first area comprises the preliminary investigations regarding the material data, while welding experiments are carried out in the second area. Because the vibration movement stretches the melt by the amplitude length, it is important for a high-quality joint that no melt break occurs. For this reason, the preliminary investigations on the one hand include experiments concerning the elongation ability of plastic melt, and on the other hand, the heat input via alternating elongation is examined. The preliminary investigations thus form the

prerequisite for the subsequent welding experiments with angled areas in the direction of vibration and are intended to demonstrate the feasibility of the process.

## 3.1 Preliminary investigations

For the preliminary investigations, a test bench was developed which enables the generation of a defined melt layer  $L_0$  and with which both a static and a dynamic load can be introduced into the melt. The basic structure is shown in Fig. 2 and comprises a heating element for the plasticizing of the material and a fluidic muscle by which the static or dynamic load of the melt is applied. The fluidic muscle provides a dynamic load of ultrasonic type with frequencies up to 100 Hz.

To determine the maximum melt elongation, the two joining partners are plasticized until a defined melt layer thickness  $L_0$  is achieved. Then both components are repositioned and joined at low pressure in order to minimize the squeezing flow of the melt into the weld bead. Subsequently, one component is pulled away from the other component at high speed. The melt tear-off  $L_t$  is then detected with a high-speed camera (Fig. 3).

As shown in Fig. 4, vibration welding of plastic components with angled areas in the direction of vibration poses two challenges. On the one hand, there is the danger that the initially generated melt is displaced by the oscillating movement and that unmelted areas of the components collide. This collision must be avoided in order to prevent unacceptable loading of the drive unit.

The maximum selectable amplitude without collision of unmelted material can be calculated using the trigonometric functions (see Fig. 5). As Fig. 5 shows, even small melt layer thicknesses of 0.25 mm can compensate angle-dependent amplitudes of 0.25 mm (joining angle  $90^\circ$ ) up to an amplitude of 0.5 mm (joining angle  $30^\circ$ ). On the other hand, the melt must accommodate the expansion due to the vibration movement without tearing off the melt film. The initial melt layer thickness  $L_0$  in combination with the determined elongation ability of the plastic melt then limits the maximum adjustable amplitude.

To evaluate the heat input by alternating elongation, one joining part is moved away from and towards the other joining

**Fig. 2** Experimental setup of the preliminary investigations

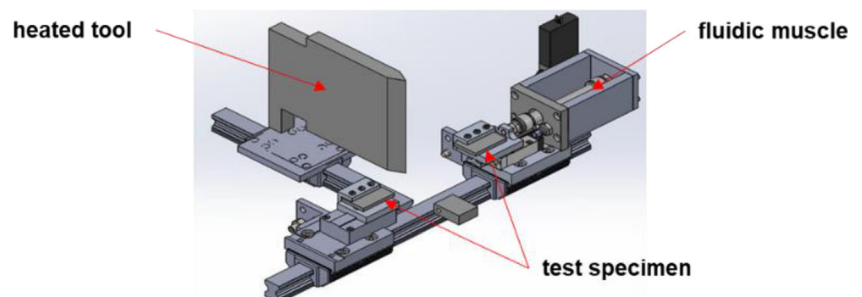
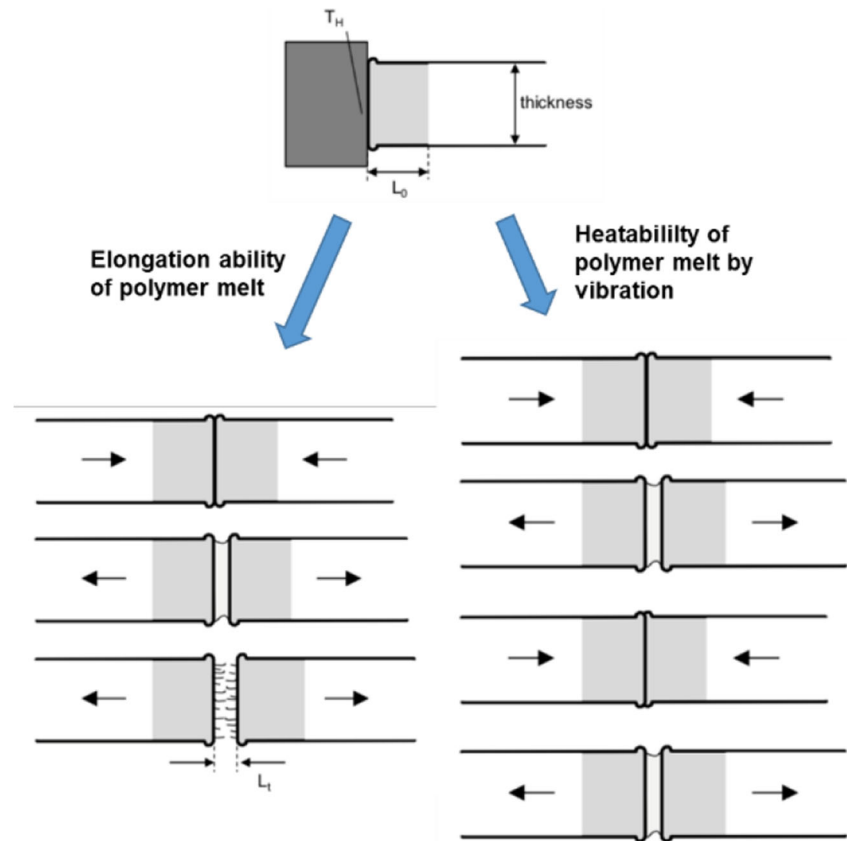


**Fig. 3** Schematic representation of the elongation analysis of polymer melt (left) and the investigations regarding heat input via alternating elongation (right)



part at different frequencies (cf. Fig. 3). Afterwards, the heat input is checked by microscopic images of the heat-affected zone and by analysis of the temperature development in the weld seam. For material data acquisition, semi-crystalline (polypropylene, polyamide 6), amorphous (acrylonitrile-butadiene-styrene-copolymer, polystyrene, polycarbonate) and fiber-reinforced thermoplastics (PP-LGF30, PP-

GF30, PA6-GF30) are investigated with regard to the elongation ability of polymer melt and heat input by alternating elongation. To determine the elongation ability and the heat input, test specimens with the dimensions  $40 \times 30 \times 2 \text{ mm}^3$  were used, which were produced at the research institute by injection molding and then mechanically processed.

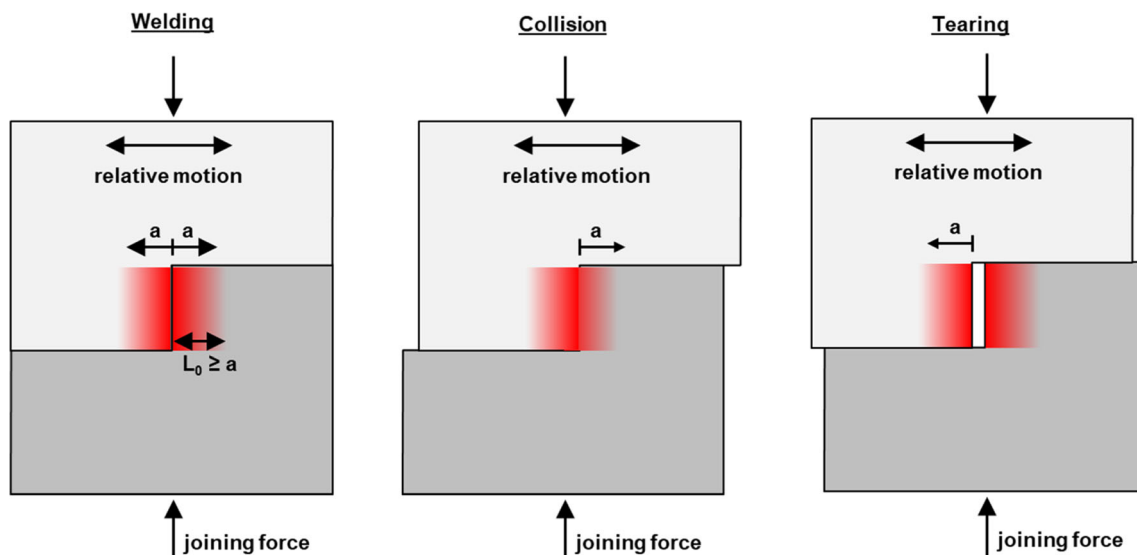
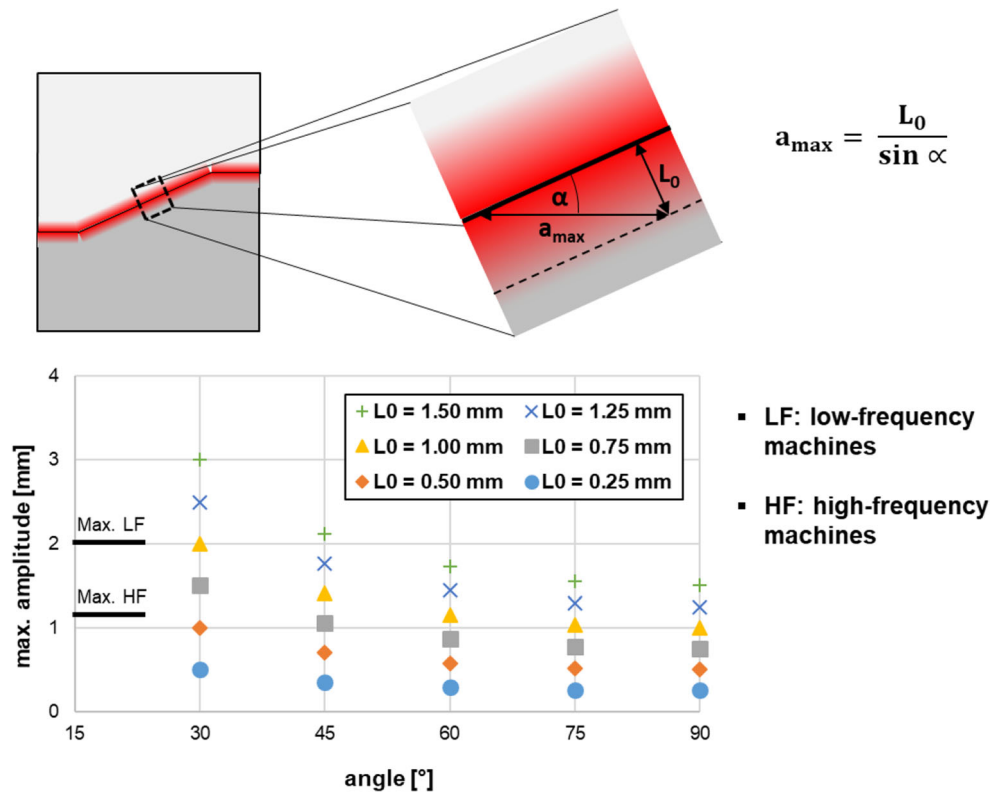


**Fig. 4** Challenges of vibration welding with angled areas in vibration direction

Fig. 5 Maximum amplitude to avoid melt tear-off



### 3.2 Welding experiments

A linear vibration welding machine with integrated IR preheating unit is used for the welding experiments. Amplitudes of 0.35 to 1 mm (peak-to-peak 0.7 to 2 mm) at frequencies up to 240 Hz (working frequency of approx. 230 Hz for the investigations carried out) can be realized with this machine. The emitters are 10 short-wave twin-tube infrared emitters, which can be individually adjusted with regard to

emitter power and irradiation duration, allowing homogeneous initial melt layer thicknesses to be set even for components with different distances to the emitters. Injection-molded rectangular plates ( $130 \times 70 \times 4 \text{ mm}^3$ ) are used for the welding experiments, which are mechanically adapted to the corresponding joining zone geometry. The resulting test specimens consist of a flat surface and an angled area. The angle between flat and angled area (joining angle) was successively increased from a  $30^\circ$  joining angle to an angle of  $45^\circ$  during the course

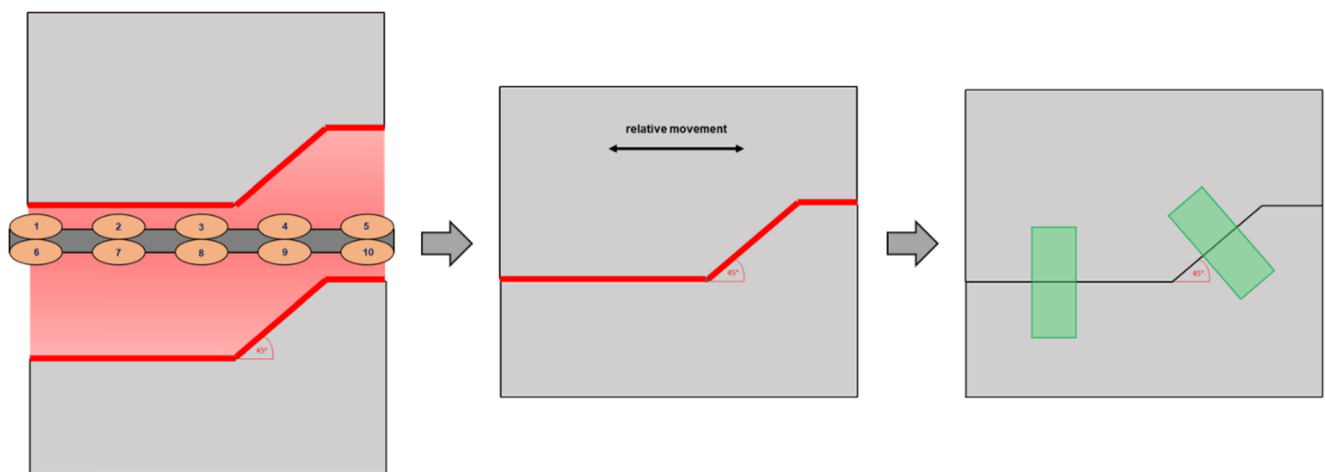


Fig. 6 Schematic representation of alternating elongation welding (left: generation of the homogeneous, initial melt layer by IR preheating; middle: heat input by vibration movement; right: specimen removal in the angled and flat areas)

of the investigations. This gradually reduces the proportion of heat input due to shear dissipation and increases the proportion of heat input due to elongation dissipation. Figure 6 shows the principle sequence of alternating elongation welding and the schematic representation of the specimen geometry. The welding experiments focus on amorphous (PC-ABS blend) and semi-crystalline materials (PP, PA6).

## 4 Results

Subsequently, the results of the elongation tests of polymer melt, the tests concerning the heat input via alternating elongation, and the welding tests on specimens with varying joining angles are presented.

### 4.1 Elongation ability of polymer melt

As already described, in order to determine the elongation ability of the plastic melt, first, a melt layer  $L_0$  is produced by contact heating at the heating element and the plasticized surfaces are joined at low pressure (the resulting weld seam then had the thickness of  $2 \times L_0$ ). The aim is to minimize the displacement of the melt into the weld bead. In the first step of the investigations, the change of the melt layer thickness with increasing heating times is investigated ( $L_t$ : melt tear-off). On this basis, tests are carried out to determine the maximum elongation ability of molten plastic. The investigations show that polymer melt has a high elongation ability, but that this depends strongly on the material and the fillers. The melt layers of non-reinforced materials can be stretched by their own thickness and beyond (cf. Figure 7). The melt layers of fiber-reinforced thermoplastics, on the other hand, can be stretched to a lesser extent until the melt tears-off. Furthermore, the maximum melt elongation  $\varepsilon_t$  of non-reinforced materials increases with increasing melt film thickness  $L_0$ . This effect does not occur with reinforced materials.

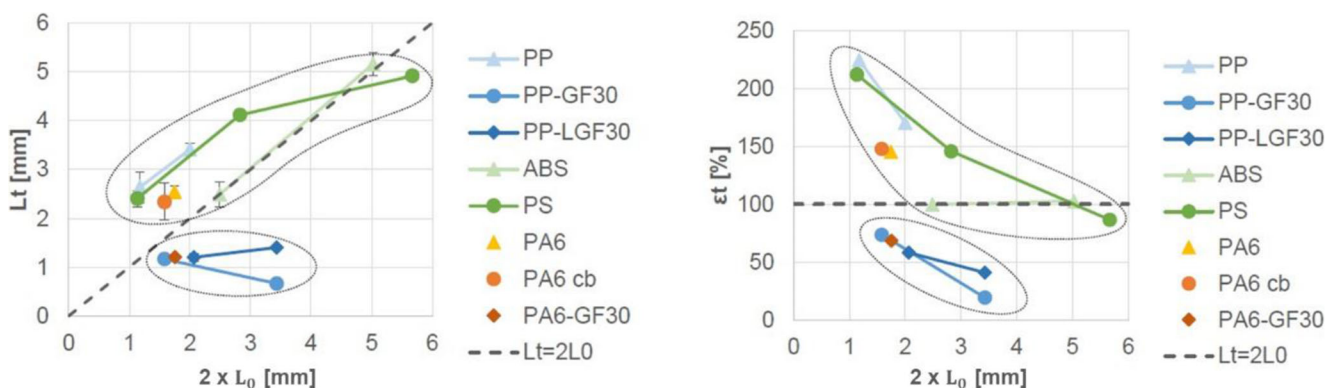


Fig. 7 Elongation ability of polymer melt

As already described, the resulting melt layer thickness limits the entire subsequent welding process. Therefore, after IR preheating, the melt layer must be sufficiently large to avoid an impermissible lifting movement on the one hand and to avoid the tearing off of the melt film on the other hand. The maximum amplitude then results from the equation in Fig. 5 (maximum amplitude without collision of the components) and the following equation:

$$a_{\max} = \frac{0.5 \cdot L_t}{\sin \alpha}$$

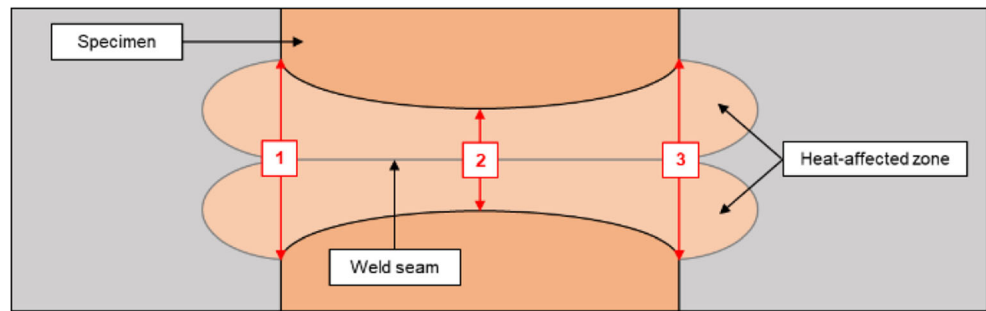
### 4.2 Heat input through alternating elongation

In order to investigate the heat input through alternating elongation at the mobile hot plate welding machine, the molten boundary layer was dynamically loaded with different frequencies. The examined frequencies are 50 and 100 Hz (minimum and maximum frequency of the pneumatic muscle). In the first step of the investigations, the heat-affected zones of loaded and unloaded samples were analyzed microscopically in order to show the heat input by alternating elongation. Figure 8 shows schematically the determination of the width of the heat-affected zone and the typical structure of a weld seam. The weld seams of loaded and unloaded seams do not differ in terms of structure, but only in the width of the heat-affected zone.

Subsequently, the surface temperature of loaded and unloaded samples is determined at different times with a thermal imaging camera. Differences in the cooling behavior of the specimen surfaces are determined and a temperature increase due to the dynamic load inside the weld seam can be inferred. As an example, the determination of the cooling rates of loaded and unloaded welds is shown in Fig. 9.

The microscopic examinations showed that the heat-affected zone of the loaded weld seams was wider compared with the width of the unloaded seams. In addition, the

**Fig. 8** Schematic representation of a typical hot plate weld seam and determination of the heat-affected zone width

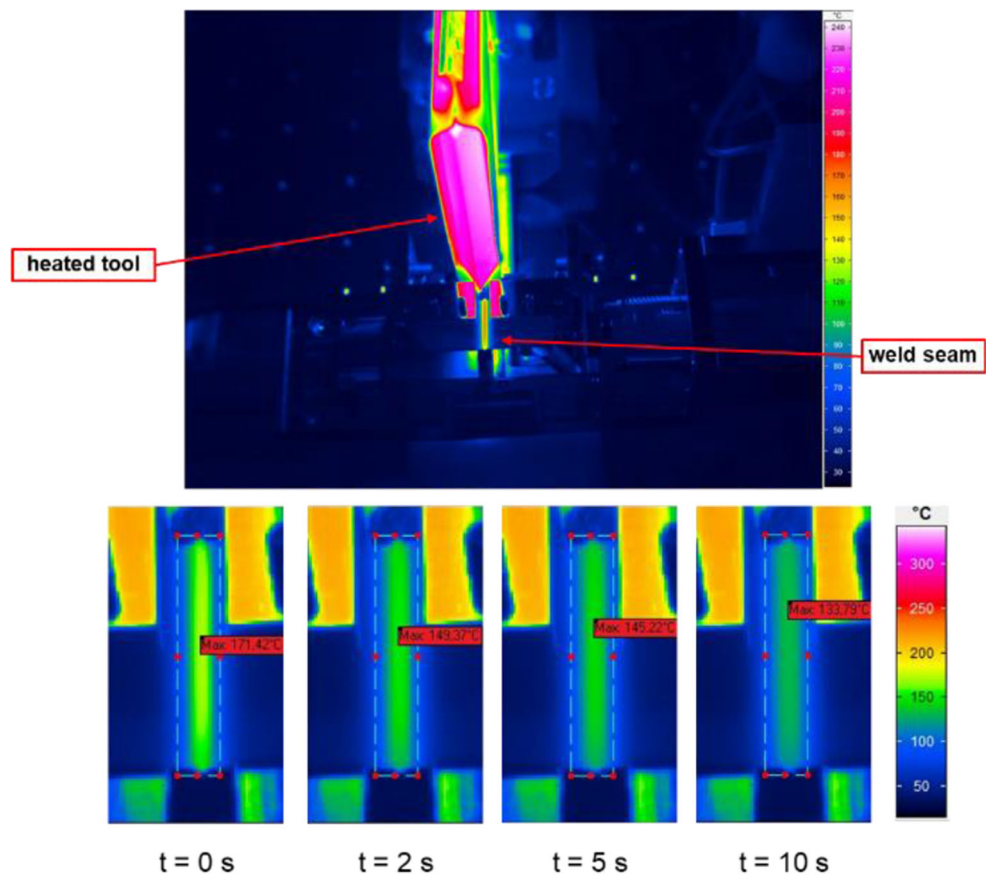


dynamically loaded weld seams cool down slower. This correlation can be observed for reinforced and non-reinforced materials, but this effect occurs to a greater extent in non-reinforced plastics. This suggests that heat is introduced into the materials via elongation dissipation. Figure 10 shows the temperature difference between the weld seam surface at the beginning of the joining process and after a time of 10 s, for unloaded and loaded components. Here, it can be seen that the dynamically loaded weld seams cool down more slowly. This suggests that heat is introduced into the materials via elongation dissipation. This effect can be observed for reinforced and non-reinforced materials but occurs to a greater extent in non-reinforced plastics, especially polypropylene.

### 4.3 Welding experiments

During the vibration welding experiments, specimens were tested with a flat surface and an angled area (cf. Figure 6). Initially, a joining angle of 30° was investigated, which was successively increased to evaluate possible process limits. The process parameters include the amplitude, the frequency with which the vibrating head is excited, the joining pressure, the welding time, and the initial melt layer thickness resulting from the IR preheating. The working frequency is limited on the machine side by the weight of the clamping tool. Due to the fact that the investigations were carried out with a high-frequency machine and a tool with a low mass, the operating

**Fig. 9** Determination of the cooling behavior of unloaded and dynamically loaded weld seams



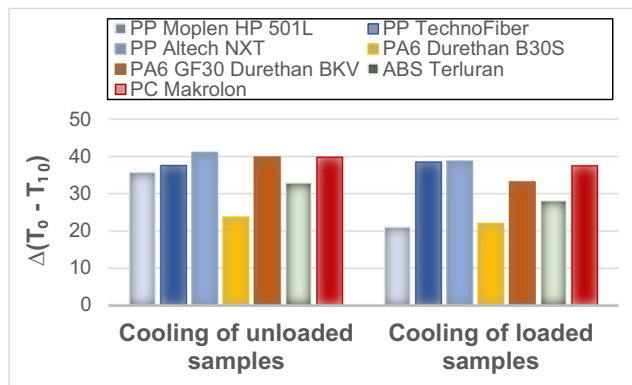


**Fig. 10** Cooling behavior of dynamically loaded and unloaded weld seams

frequency was above 200 Hz. In order to compensate the oscillating movement and therefore to avoid a collision of non-plasticized areas and to prevent a tearing off of the melt, the welding tests are carried out with low amplitudes. The joining pressure was adjusted according to the joining angle so that pressures between 0.5 and 5 MPa were achieved in the plane and in the angled areas. By varying the IR parameters, different initial melt thicknesses could be generated ( $0.3 \text{ mm} \leq L_0 \leq 0.7 \text{ mm}$ ). The smallest initial melt layer was only so large that there was no collision of the unmelted areas. After reaching the third, stationary phase, the vibration was stopped and the process could be terminated. The welded joints in the flat and in the angled areas were then characterized by mechanical and microscopic examinations. As already described, welding tests were carried out using various materials (PP, PC-ABS, PA6) with different melt viscosities in order to determine their influence on the welding process. PP had the highest and PA6 the lowest melt viscosity of the materials under consideration. The melt viscosity of PC-ABS can be classified between the viscosities of the other two materials [26].

During the welding tests, the main variables tested were joining pressure and the initial melt layer thickness. For welds with joining angles of  $30^\circ$  as well as for welds with a joining angle of  $45^\circ$ , it was determined that the weld strength was less influenced by the joining pressure than by the initial melt layer thickness due to IR preheating. Figure 11 shows the tensile strength of welded  $30^\circ$  specimens as a function of the initial melt layer thickness. The investigations regarding the weld strength showed that for welds with an initial melt layer thickness  $L_0$  of 0.3 mm as well as for welds with a melt layer thickness  $L_0$  of 0.7 mm, cohesive joints could be generated. However, a significant difference in weld strength could be identified between welds with different initial melt layers. The increase of the initial melt layer resulted in an improved bond strength for PP with a comparatively high melt viscosity and for the materials with a lower melt viscosity.

This correlation can be explained exemplarily by the microscopic images of the PP specimens in Fig. 12. On the one

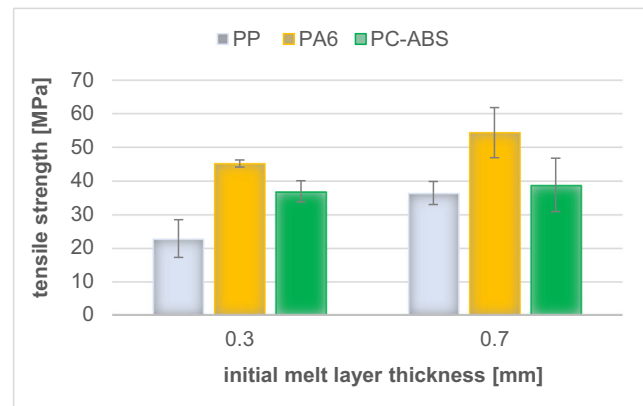


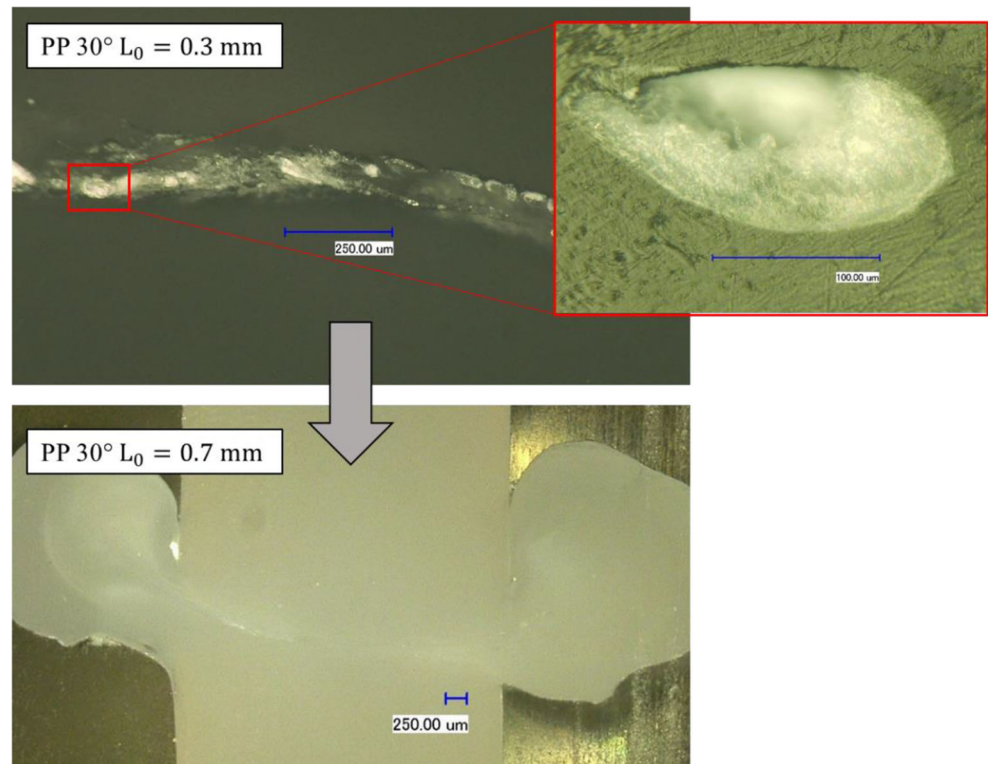
**Fig. 11** Weld seam strength of the angled areas in relation to the initial melt layer (joining angle  $30^\circ$ )

hand, the illustrations show weld seams with a low initial melt layer thickness and, on the other hand, the weld seam with a comparatively high initial melt layer. In the welds with a low melt layer, material was forced into the bead by the joining pressure and the vibration movement before additional material was plasticized through the alternating elongation. The remaining melt film could not be sufficiently stretched and sheared. As a result, shear and elongation dissipation are reduced. The vibration movement in combination with the small melt layer also creates vacuoles. These structures acted as defects in the material and led to a lower weld strength. For  $30^\circ$  welds with a larger initial melt layer, these defects could no longer be identified respectively only to a very small extent. In this case, the melt in the joining zone was large enough to be heated by shearing and elongation for additional plastification. Comparable results were also found in the microscopic examinations of the two other materials.

As already described, the heat input in conventional vibration welding takes place via shearing of the melt. In vibration welding of angled areas, the energy input occurs through superimposed shear and strain dissipation. While the proportion of shear dissipation predominates for smaller joining angles, the proportion of elongation dissipation increases as the joining angle rises (complete elongation dissipation without shear dissipation would occur at a joining angle of  $90^\circ$ ). For this reason, the joining angle was successively increased to  $45^\circ$ . In this context, Fig. 13 shows the weld seam strength of the angled areas in relation to the initial melt layer at a joining angle of  $45^\circ$ . Similar to the results of the welding tests with an angle of  $30^\circ$ , an increased melt layer proved to be a more decisive factor for a high weld quality than the applied joining pressure was. Higher weld seam strengths could be obtained for all three investigated materials by previously generating a larger initial melt layer by IR preheating. This effect had a stronger influence on materials with a low initial melt viscosity, due to the increased melt being pressed out of the joining zone by the vibration and joining pressure. This means PP can be welded at a joining angle of  $45^\circ$  with a tensile strength



**Fig. 12** Weld seam in the angled area with different initial melt layer thicknesses (joining angle 30°)



comparable with the base material. For the thinner melt layer and the additional squeeze flow into the bead, the weld strengths of PA6 and PC-ABS are below the base material strength level (welding factor < 1).

While the 45° weld seams of the PP specimens did not exhibit any visible anomalies, the welded joints of other materials showed clear defects. The comparison between the welds of PA6 at the angles of 30° and 45° showed significant differences. The microscopic examinations of the PA6 welds with different initial melt thicknesses are shown in Fig. 14. Both the welds with a low initial melt layer and those with a higher melt layer thickness exhibited conspicuous structures in the joining zone. However, the weld seams with a lower

initial melt layer showed significantly fragmented structures with significantly larger vacuoles. These defects caused the lower tensile strength compared with weld seams with higher melt layer thickness.

To evaluate welded joints, the so-called welding factor is often calculated. This indicates the ratio of the weld seam strength to the base material strength and should ideally be 1. In this case, the weld seam is not a weak part of the entire component. Table 1 shows the maximum welding factors of the welded joints in the angled areas using optimized welding parameters. For the comparison between angled and flat areas, the welding factors of the flat area are also given. The welding tests showed that high-quality welds can be realized for the joining angle of 30°. The joints showed weld seam qualities which were comparable with conventional vibration welding. For the 45° joining angle, a different result could be determined. For the PP specimens, high welding factors could nevertheless be achieved, while for the PA6- and PC-ABS-welds lower welding factors were obtained. This correlation can be explained by the lower melt viscosity of the materials. The viscous melt of the PA6 and the PC-ABS was pressed out of the joining zone by the applied joining pressure and the vibration movement. As a result of this process, shear and elongation dissipation had a reduced effect and less heat energy was introduced into the material. At lower joining angles, this effect occurred to a lesser extent and affected the weld quality less. Despite the comparatively

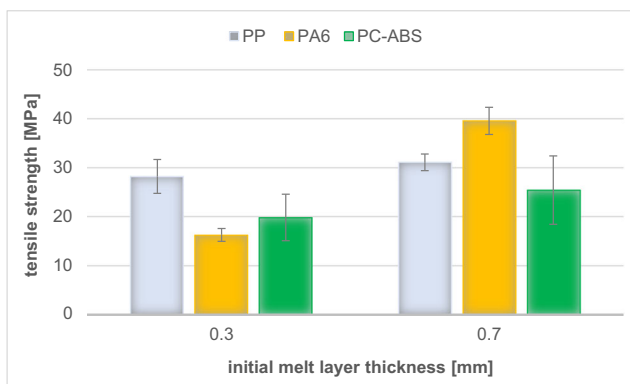


**Fig. 13** Weld seam strength of the angled areas in relation to the initial melt layer (joining angle 45°)

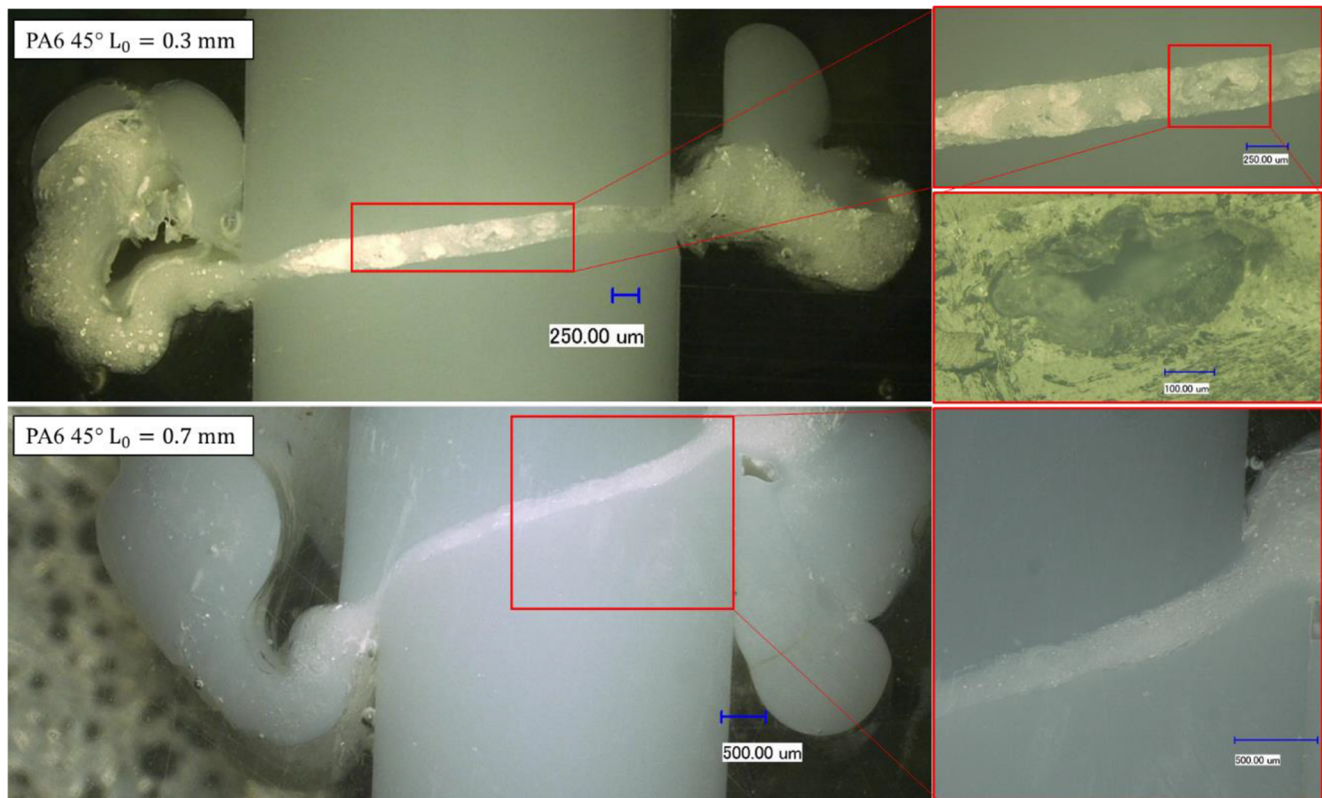


**Fig. 14** Weld seam in the angled area at different initial melt layer thicknesses (joining angle 45°)

low welding factors, the weld seams of the 45° components show a cohesive material bonding and solid weld seam strengths.

Consequently, the described process can compete with IR welding in terms of weld strength in the three-dimensional areas. In addition to the process-technical side, the investigations also showed that the combined method of vibration welding with infrared preheating is also an alternative to IR welding in terms of economy. While comparable components can be joined within 52 s using IR welding [27], welding with the presented method takes 38 s. As a result, the method can compete with IR welding in terms of both process technology and economy, and industrial application can be economically viable.

**Table 1** Welding factors of the different materials with varying joining angles (joining angle 0° denotes the welding factor in the flat areas)

Welding factor $\left(\frac{\text{weld strength}}{\text{material strength}}\right)$	Material			
		PP	PA6	PC-ABS
Joining angle	0°	1	0.9	0.7
	30°	1	0.7	0.7
	45°	0.9	0.5	0.5

## 5 Summary and conclusion

The welding of three-dimensional joining seams with short cycle times has long been studied, and the investigations presented here are intended to add to that literature. Vibration welding is known for short cycle times, but deviations from the flat joining zone are a challenge for the process. For angled areas in the direction of vibration, only a small amount of heat energy is introduced into the joining zone, often resulting in a poor joint. During the investigations presented here, experiments were carried out to introduce additional heat into a previously plasticized initial molten layer by introducing vibration movements. The heat is then introduced by superimposed shear and elongation dissipation. For this purpose, preliminary investigations were carried out with regard to the elongation ability of polymer melt and with regard to the heat input by elongation dissipation. The aim of the preliminary investigations was to demonstrate the general feasibility of the process and to enable further investigations. In order to introduce as much heat as possible into the initial melt layer, it is essential that the melt does not tear off during elongation. The investigations carried out showed that polymer melt has a high elongation ability in principle, but that this is influenced by the material itself and by the additives contained in the material. Unreinforced melt, for example, can be stretched by its own width, while the fiber-reinforced melt only tolerates

significantly lower elongations before the melt tears off. The investigations concerning heat input into polymer melt by elongation dissipation showed that the elongation of the melt introduced additional energy and thus enabled further welding experiments.

The subsequent welding experiments showed that both flat and angled areas can be welded using the method described. The bond strength in the angled areas depends strongly on the joining angle, the amplitude, the initial melt layer thickness, and the material-specific melt viscosity. In small initial melt layers, a large part of the melt is pressed into the bead by the vibration and the applied joining pressure. As a result, the amount of melt that can be further heated by shear and elongation dissipation is too low to generate a high-quality weld. This effect can be counteracted by increasing the initial melt layer thickness after IR-preheating. For materials with comparatively low viscosity melts, this effect is more pronounced and has a negative effect on weld strength at higher joining angles, despite the larger initial melt layers.

**Acknowledgments** Open Access funding provided by Projekt DEAL. The IGF Project 19031N of the research association “Forschungsvereinigung Schweißen und verwandte Verfahren e.V. des DVS. Aachener Straße 172. 40223 Düsseldorf” was, on the basis of a resolution of the German Bundestag, promoted by the German Ministry of Economic Affairs and Energy via AiF within the framework of the program for the promotion of joint industrial research and development (IGF).

**Abbreviations**  $L_0$ , initial melt layer thickness after IR-preheating;  $L_t$ , melt tear-off;  $\varepsilon_t$ , maximum melt elongation;  $a_{\max}$ , maximum amplitude;  $\alpha$ , joining angle; LF, low frequent machine; HF, high frequent machine; PP, polypropylene; PA6, polyamide 6; ABS, Acrylnitril-Butadien-Styrol-Copolymer; PC, polycarbonate; IR, infrared;  $f_w$ , welding factor;  $\sigma_m$ , material strength;  $\sigma_w$ , weld strength

**Open Access** This article is licensed under a Creative Commons Attribution 4.0 International License, which permits use, sharing, adaptation, distribution and reproduction in any medium or format, as long as you give appropriate credit to the original author(s) and the source, provide a link to the Creative Commons licence, and indicate if changes were made. The images or other third party material in this article are included in the article's Creative Commons licence, unless indicated otherwise in a credit line to the material. If material is not included in the article's Creative Commons licence and your intended use is not permitted by statutory regulation or exceeds the permitted use, you will need to obtain permission directly from the copyright holder. To view a copy of this licence, visit <http://creativecommons.org/licenses/by/4.0/>.

## References

- Ehrenstein GW (2004) Handbuch Kunststoffverbindungstechnik. München, Carl Hanser Verlag
- Potente H (2004) Fügen von Kunststoffen. München, Carl Hanser Verlag
- Potente H, Karger O, Müller A (2004) In Kombination - Durch IR-Vorwärmung kein Abrieb beim Vibrationsschweißen. *Plastverarbeiter* 55:54–56
- Heim HP et al (2006) Abrieb - und Fusselminimierung beim Vibrationsschweißen. *Kunststoffe* 3:45–48
- Kazmirzak W et al (2008) HE-Schweißen mit Ultraschall. *Join Plast. Bd. 08*, 01
- Friedrich N, Schöppner V (2012) Zykluszeitreduzierung ohne Qualitätsverlust beim Heizelementschweißen durch Zwangskühlung mittels Druckluft. *Join Plast* 12:2
- Stokes VK (1986) Vibration welding of thermoplastics part 1: phenomenology of the welding process. Technical information series, General Electric, Corporate research and development, New York
- Potente H et al (1987) Eine Analyse des Vibrationsschweißens. *Kunststoffe* 77:711–716
- Stokes VK (1988) Vibration welding of thermoplastics. Part II: analysis of the welding process. *Polymer Engineering and Science*, New York
- Schlarb A (1989) Zum Vibrationsschweißen von Polymerwerkstoffen. Dissertation Universität Gesamtschule Kassel, Herausgeber: Institut für Werkstofftechnik, Ehrenstein GW
- Kaiser H (1992) Prozeßanalyse und Prozessführung beim linearen Vibrationsschweißen von Kunststoffen. Düsseldorf: DVS-Verlag
- Ehrenstein GW, Künkel R (2006) Strukturbildung in der Schweißnaht beim Vibrationsschweißen. *Schweißen und Schneiden* 58:345–349
- Grewell D, Benatar A (2009) Comparison of orbital and linear vibration welding of thermoplastics: *Polymer Engineering and Science* 2009:1410–1420
- Grewell D, Benatar A (2007) Welding of plastics: fundamentals and new developments. Carl Hanser Verlag, München, *International Polymer Processing XXII*:43–60
- DVS AG W 4 (2012) Taschenbuch DVS-Merkblätter und -Richtlinien. Berlin: Beuth Verlag GmbH
- Uebbing M (1995) Berechnungsmöglichkeit und Qualitätssicherung beim Vibrationsschweißen. Düsseldorf: DVS-Verlag
- Rotheiser J (2009) Joining of plastics. Carl Hanser Verlag. München
- Gehde M, Friedrich S (2015) On the influence of the oscillation direction during linear vibration welding. *Joining Plastics* 2:99–105
- Bates PJ, Dai XY, Wu C-Y (2005) Vibration welding non-planar surfaces. ANTEC
- Strohfuss W (2007) Infrarot unterstütztes Vibrationsschweißen - Ein in der Praxis eingeführtes Standardverfahren. Bde. *Kunststoff-Motorbauteile Forum*
- Rattke M, Natrop J (2007) Infrarot erwärmung in der Kunststofftechnik. Düsseldorf: DVS-Verlag
- Brahm J (2012) Neue Maßstäbe bei Strahlung und Reibung. München: Carl Hanser Verlag. *Kunststoffe* 3:84–87
- Fuhrich R (2011) Strahlungserwärmung beim Kunststoffschweißen mit Infrarotstrahlung. Chemnitz: Abschlussbericht AiF-IGF-Vorhaben 15971 BR
- Menges G et al (2002) *Werkstoffkunde Kunststoffe*, München, Carl Hanser Verlag, 5. Völlig überarbeitete Auflage
- Cerbe G, Wilhelms G (2008) Technische Thermodynamik, Theoretische Grundlagen und praktische Anwendungen. München, Carl Hanser Verlag. 15. Aktualisierte Auflage
- Schröder T (2018) *Rheologie der Kunststoffe*. München, Carl Hanser Verlag
- Friedrich S (2019) *Schweißen von Kunststoffen in der Großserienfertigung*. Chemnitz, Technomer

**Publisher's note** Springer Nature remains neutral with regard to jurisdictional claims in published maps and institutional affiliations.